Enhancement of Molecular Quadratic Hyperpolarizabilities in Ruthenium(II) 4,4′-Bipyridinium Complexes by N-Phenylation

Benjamin J. Coe*,[†] James A. Harris,[†] Lisa J. Harrington,[†] John C. Jeffery,[‡] Leigh H. Rees,[‡] Stephan Houbrechts,[§] and André Persoons[§,||]

Department of Chemistry, University of Manchester, Oxford Road, Manchester M13 9PL, U.K., Department of Chemistry, University of Bristol, Cantock's Close, Bristol BS8 1TS, U.K., Laboratory of Chemical and Biological Dynamics, Center for Research on Molecular Electronics and Photonics, University of Leuven, Celestijnenlaan 200D, B-3001 Leuven, Belgium, and Optical Sciences Center, University of Arizona, Tucson, Arizona 85721

Received November 7, 1997

The new compounds *N*-phenyl-4,4′-bipyridinium (PhQ^+), *N*-(4-acetylphenyl)-4,4′-bipyridinium ($4\text{-}AcPhQ^+$), and *N*-(2,4-dinitrophenyl)-4,4′-bipyridinium ($2,4\text{-}DNPhQ^+$), together with the known ligand *N*-methyl-4,4′-bipyridinium (MeQ^+), have been used to prepare a series of Ru(II) complex salts *trans*-$[Ru(NH_3)_4(L^D)(L^A)](PF_6)_3$ [$L^D = NH_3$ and $L^A = MeQ^+$ (**1**), PhQ^+ (**2**), $4\text{-}AcPhQ^+$ (**3**), or $2,4\text{-}DNPhQ^+$ (**4**); L^D = 4-(dimethylamino)pyridine (dmap) and $L^A = PhQ^+$ (**7**) or $4\text{-}AcPhQ^+$ (**11**); L^D = 1-methylimidazole (mim) and $L^A = PhQ^+$ (**8**) or $4\text{-}AcPhQ^+$ (**12**); L^D = 4-(dimethylamino)benzonitrile (dmabn) and $L^A = PhQ^+$ (**9**) or $4\text{-}AcPhQ^+$ (**13**); L^D = phenothiazine (PTZ) and $L^A = PhQ^+$ (**10**) or $4\text{-}AcPhQ^+$ (**14**)]. These complexes display intense, visible metal-to-ligand charge-transfer (MLCT) absorptions, due to $d\pi(Ru^{II}) \rightarrow \pi^*(L^A)$ excitations. The MLCT energy decreases as the acceptor strength of L^A increases, in the order $MeQ^+ < PhQ^+ < 4\text{-}AcPhQ^+ < 2,4\text{-}DNPhQ^+$, and/or as the donor strength of L^D increases, in the order PTZ < dmabn < NH_3 < mim < dmap. X-ray crystal structure determinations have been carried out for $[PhQ^+]Cl\cdot 2H_2O$ and *trans*-$[Ru(NH_3)_4(PhQ^+)(PTZ)](PF_6)_3\cdot Et_2O$ (**10**·Et_2O). $[PhQ^+]Cl\cdot 2H_2O$, chemical formula $C_{16}H_{17}ClN_2O_2$, crystallizes in the triclinic system, space group $P\bar{1}$, with $a = 7.675(2)$ Å, $b = 9.895(2)$ Å, $c = 10.175(2)$ Å, $\alpha = 96.003(1)°$, $\beta = 104.74(2)°$, $\gamma = 90.398(1)°$, and $Z = 2$. **10**·Et_2O, chemical formula $C_{32}H_{44}F_{18}N_7OP_3RuS$, crystallizes in the triclinic system, space group $P\bar{1}$, with $a = 10.310(3)$ Å, $b = 10.698(2)$ Å, $c = 20.986(4)$ Å, $\alpha = 95.09(2)°$, $\beta = 91.49(2)°$, $\gamma = 105.53(2)°$, and $Z = 2$. The dihedral angles between the two pyridyl rings of the 4,4′-bipyridinium unit are 19.8° in $[PhQ^+]Cl\cdot 2H_2O$ and 2.6° in **10**·Et_2O. Molecular first hyperpolarizabilities β of the complex salts, obtained from hyper-Rayleigh scattering measurements at 1064 nm, are in the range $(698-1214) \times 10^{-30}$ esu. Static hyperpolarizabilities β_0 derived by using the two-level model are very large, with *trans*-$[Ru(NH_3)_4(4\text{-}AcPhQ^+)(dmap)](PF_6)_3$ (**11**) having the largest at 410×10^{-30} esu. When the MLCT absorption is sufficiently far from the second harmonic at 532 nm, both β and β_0 increase as the absorption energy decreases.

Introduction

The development of novel optoelectronic and photonic technologies requires organic materials possessing nonlinear optical (NLO) properties.[1] A thorough understanding of molecular hyperpolarizabilities is a prerequisite to the rational design and synthesis of efficient NLO chromophores for incorporation into active bulk structures. Structure−property correlations for the first (quadratic) hyperpolarizability β of purely organic compounds are now at an advanced stage of development,[1] but the molecular basis for NLO effects in organotransition metal complexes is relatively poorly understood.[2] Only very recently have studies begun to address this deficiency.[3−8]

Several reports concerning the quadratic NLO properties of ruthenium organometallic σ-acetylide[9] or allenylidene[10] complexes have appeared. We have chosen to investigate the NLO

* Author to whom correspondence should be addressed (e-mail, b.coe@man.ac.uk).
[†] University of Manchester.
[‡] University of Bristol.
[§] University of Leuven.
[||] University of Arizona.

(1) (a) *Nonlinear Optical Properties of Organic Molecules and Crystals*; Chemla, D. S., Zyss, J., Eds.; Academic Press: Orlando, 1987; Vols. 1 and 2. (b) *Materials for Nonlinear Optics: Chemical Perspectives*; Marder, S. R., Sohn, J. S., Stucky, G. D., Eds.; ACS Symposium Series 455; American Chemical Society: Washington, DC, 1991. (c) *Molecular Nonlinear Optics*; Zyss, J., Ed.; Academic Press: New York, 1994. (d) Marder, S. R.; Kippelen, B.; Jen, A. K.-Y.; Peyghambarian, N. *Nature* **1997**, *388*, 845.

(2) (a) Marder, S. R. In *Inorganic Materials*; Bruce, D. W., O'Hare, D., Eds.; Wiley: Chichester, U.K., 1992. (b) Kanis, D. R.; Ratner, M. A.; Marks, T. J. *Chem. Rev.* **1994**, *94*, 195. (c) Long, N. J. *Angew. Chem., Int. Ed. Engl.* **1995**, *34*, 21.

(3) (a) Behrens, U.; Brussaard, H.; Hagenau, U.; Heck, J.; Hendrickx, E.; Körnich, J.; van der Linden, J. G. M.; Persoons, A.; Spek, A. L.; Veldman, N.; Voss, B.; Wong, H. *Chem. Eur. J.* **1996**, *2*, 98. (b) Hagenau, U.; Heck, J.; Hendrickx, E.; Persoons, A.; Schuld, T.; Wong, H. *Inorg. Chem.* **1996**, *35*, 7863.

(4) (a) Di Bella, S.; Fragala, I.; Ledoux, I.; Marks, T. J. *J. Am. Chem. Soc.* **1995**, *117*, 9481. (b) Lacroix, P. G.; Di Bella, S.; Ledoux, I. *Chem. Mater.* **1996**, *8*, 541.

(5) Nguyen, P.; Lesley, G.; Marder, T. B.; Ledoux, I.; Zyss, J. *Chem. Mater.* **1997**, *9*, 406.

(6) Cummings, S. D.; Cheng, L.-T.; Eisenberg, R. *Chem. Mater.* **1997**, *9*, 440.

(7) (a) Alain, V.; Fort, A.; Barzoukas, M.; Chen, C.-T.; Blanchard-Desce, M.; Marder, S. R.; Perry, J. W. *Inorg. Chim. Acta* **1996**, *242*, 43. (b) Wu, Z.; Ortiz, R.; Fort, A.; Barzoukas, M.; Marder, S. R. *J. Organomet. Chem.* **1997**, *528*, 217.

S0020-1669(97)01411-0 CCC: $15.00
Published on Web 06/09/1998

properties of ruthenium(II) ammine complexes of pyridyl ligands, because these combine ideal, well-understood redox and charge-transfer absorption properties with synthetic versatility. The recently developed hyper-Rayleigh scattering (HRS) technique[11] allows the determination of β values of such complex salts. Initial studies have shown that *trans*-$\{Ru(NH_3)_4\}^{2+}$ complexes can possess large static hyperpolarizabilities β_0 which are associated with intense, low-energy metal-to-ligand charge-transfer (MLCT) absorptions.[12] The d^6 Ru(II) centers behave as powerful π donors, and the linear absorption and, hence, NLO properties are readily tuned via ligand modifications. Complexes of the *N*-methyl-4,4′-bipyridinium (MeQ^+) ligand have especially large β_0 values because MeQ^+ is a particularly effective π acceptor.

The present objectives of our research are fundamental in nature and include the maximization of β_0, together with the development of a detailed understanding of the origins of the NLO responses in Ru(II) 4,4′-bipyridinium chromophores. By analogy with dipolar organic molecules,[1] it is anticipated that the magnitude of the first hyperpolarizability will be increased by improving the π-electron-accepting ability of the 4,4′-bipyridinium ligand. The *N*,*N*′-diphenyl-4,4′-bipyridinium dication is more readily reduced than its dimethyl analogue by 150 mV,[13] as a result of extended conjugation. We hence reasoned that the *N*-phenyl-4,4′-bipyridinium (PhQ^+) ligand should be a better π acceptor than MeQ^+, and that substitution of the phenyl ring with electron-withdrawing groups will further enhance the acceptor strength. Although data for various highly NLO active pyridinium or *N*-methylpyridinium salts is available,[14] surprisingly it appears that no *N*-phenylpyridinium compounds have been investigated in this context. Some of the results reported herein have appeared recently as a preliminary communication.[15]

Experimental Section

Materials and Procedures. $RuCl_3 \cdot 2H_2O$ was supplied by Johnson Matthey plc. The salts $[Ru^{II}(NH_3)_5(H_2O)](PF_6)_2$, *trans*-$[Ru^{II}Cl(NH_3)_4(SO_2)]Cl$, and $[Ru^{II}(NH_3)_5(MeQ^+)](PF_6)_3$ (**1**) were prepared according to published procedures.[16] $[Ru^{II}(NH_3)_5(L^A)](PF_6)_3$ [L^A = PhQ^+ (**2**) or 4-$AcPhQ^+$ (**3**)] were prepared by following the procedure reported for their MeQ^+ analogue, but using $[PhQ^+]Cl$ or [4-$AcPhQ^+$]Cl, respectively, in place of $[MeQ^+]I$. All other reagents were obtained commercially and used as supplied. Products were dried overnight at room temperature in a vacuum desiccator ($CaSO_4$) prior to characterization.

Physical Measurements. ^1H NMR spectra were recorded on a Varian Gemini 200 spectrometer, and all shifts are referenced to TMS. The fine splitting of pyridyl or phenyl ring AA′BB′ patterns is ignored, and the signals are reported as simple doublets. Elemental analyses were performed by the Microanalytical Laboratory, University of Manchester. IR spectra were obtained as KBr disks with an ATI Mattson Genesis Series FTIR instrument. UV−visible spectra were recorded using a Hewlett-Packard 8452A diode array spectrophotometer.

Cyclic voltammetric measurements were carried out using an EG&G PAR model 173 potentiostat with an EG&G PAR model 175 universal programmer. A single-compartment cell was used with the SCE reference electrode separated by a salt bridge from the Pt bead working electrode and Pt wire auxiliary electrode. HPLC grade acetonitrile was used as received, and $[N(n\text{-}C_4H_9)_4]PF_6$, twice recrystallized from ethanol and dried in vacuo, was used as supporting electrolyte. Solutions containing ca. 10^{-3} M analyte (0.1 M electrolyte) were deaerated by N_2 purging. All $E_{1/2}$ values were calculated from $(E_{pa} + E_{pc})/2$ at a scan rate of 200 mV s^{-1}.

Synthesis of *N*-(2,4-Dinitrophenyl)-4,4′-bipyridinium Chloride, [2,4-DNPhQ^+]Cl. A solution of 2,4-dinitrochlorobenzene (13.16 g, 65 mmol) and 4,4′-bipyridine (10.00 g, 64 mmol) in ethanol (250 mL) was heated at reflux for 20 h. The solvent was reduced to a small volume in vacuo, diethyl ether was added, and the precipitate was filtered off and washed with diethyl ether. The crude product was dissolved through a frit in ethanol and reprecipitated by the slow addition of diethyl ether. The golden-brown microcrystalline product was filtered off, washed with diethyl ether, and dried: 10.33 g, 42%; δ_H (D_2O) 9.35 (1 H, d, $J_{3,5}$ = 2.5 Hz, H^3), 9.22 (2 H, d, J = 7.1 Hz, C_5H_4N−Ph), 8.90 (1 H, dd, $J_{5,6}$ = 8.7 Hz, $J_{3,5}$ = 2.5 Hz, H^5), 8.79 (2 H, d, J = 6.2 Hz, C_5H_4N), 8.65 (2 H, d, J = 7.1 Hz, C_5H_4N−Ph), 8.25 (1 H, d, $J_{5,6}$ = 8.7 Hz, H^6), 7.98 (2 H, d, J = 6.4 Hz, C_5H_4N); $\nu_{as}(NO_2)$ 1548 vs, $\nu_s(NO_2)$ 1345 vs cm^{-1}. Anal. Calcd for $C_{16}H_{11}ClN_4O_4 \cdot 0.5C_2H_5OH \cdot 0.25H_2O$: C, 52.86; H, 3.78; N, 14.50; Cl, 9.18. Found: C, 52.62; H, 3.75; N, 14.40; Cl, 9.25.

Synthesis of *N*-(2,4-Dinitrophenyl)-4,4′-bipyridinium Hexafluorophosphate, [2,4-DNPhQ^+]PF_6. [2,4-DNPhQ^+]$Cl \cdot 0.5C_2H_5OH \cdot 0.25H_2O$ (452 mg, 1.17 mmol) was dissolved in water (5 mL) and filtered into stirring aqueous NH_4PF_6. The precipitate was filtered off, washed with water, and dried to afford a pale golden solid: 334 mg, 60%; δ_H (CD_3COCD_3) 9.58 (2 H, d, J = 7.2 Hz, C_5H_4N−Ph), 9.29 (1 H, d, $J_{3,5}$ = 2.5 Hz, H^3), 9.06 (1 H, dd, $J_{5,6}$ = 8.6 Hz, $J_{3,5}$ = 2.5 Hz, H^5), 8.98 (2 H, d, J = 7.2 Hz, C_5H_4N−Ph), ca. 8.80 (2 H, br, C_5H_4N), 8.61 (1 H, d, $J_{5,6}$ = 8.6 Hz, H^6), 8.16 (2 H, d, J = 6.2 Hz, C_5H_4N); $\nu_{as}(NO_2)$ 1548 vs, $\nu_s(NO_2)$ 1345 vs cm^{-1}. Anal. Calcd for $C_{16}H_{11}F_6N_4O_4P \cdot 0.5H_2O$: C, 40.27; H, 2.53; N, 11.74. Found: C, 40.06; H, 2.28; N, 11.54. A small portion of this product was dissolved in acetone and metathesized back to [2,4-DNPhQ^+]Cl by the addition of an acetone solution of $[NBu_4]Cl$. Anal. Calcd for $C_{16}H_{11}ClN_4O_4 \cdot H_2O$: C, 51.01; H, 3.48; N, 14.87; Cl, 9.41. Found: C, 51.02; H, 3.47; N, 14.71; Cl, 9.34.

Synthesis of *N*-Phenyl-4,4′-bipyridinium Chloride, [PhQ^+]Cl. A solution of [2,4-DNPhQ^+]$Cl \cdot 0.5C_2H_5OH \cdot 0.25H_2O$ (5.00 g, 12.9 mmol) and aniline (5.00 g, 53.7 mmol) in ethanol (100 mL) was heated at reflux for 3 h. The solvent was reduced to a small volume in vacuo, water was added, and the precipitate of 2,4-dinitroaniline was filtered off and washed with water. The aqueous filtrate was evaporated to dryness and then dissolved in ethanol and precipitated by the addition of diethyl ether. The pale golden microcrystalline product was filtered off, washed with diethyl ether, and dried: 3.39 g, 86%; δ_H (D_2O) 9.14 (2 H, d, J = 7.0 Hz, C_5H_4N−Ph), 8.69 (2 H, br d, C_5H_4N), 8.48 (2 H, d, J = 7.0 Hz, C_5H_4N−Ph), 7.89 (2 H, d, J = 6.3 Hz, C_5H_4N), 7.74−7.64 (5 H, c m, Ph). Anal. Calcd for $C_{16}H_{13}ClN_2 \cdot 2H_2O$: C, 63.05; H, 5.62; N, 9.19; Cl, 11.63. Found: C, 63.29; H, 5.42; N, 9.48; Cl, 11.72.

Synthesis of *N*-(4-Acetylphenyl)-4,4′-bipyridinium Chloride, [4-AcPhQ^+]Cl. A solution of [2,4-DNPhQ^+]$Cl \cdot 0.5C_2H_5OH \cdot 0.25H_2O$

(8) (a) Whittall, I. R.; Humphrey, M. G.; Houbrechts, S.; Persoons, A.; Hockless, D. C. R. *Organometallics* **1996**, *15*, 5738. (b) Whittall, I. R.; Cifuentes, M. P.; Humphrey, M. G.; Luther-Davies, B.; Samoc, M.; Houbrechts, S.; Persoons, A.; Heath, G. A.; Bogsányi, D. *Organometallics* **1997**, *16*, 2631.

(9) (a) Whittall, I. R.; Humphrey, M. G.; Persoons, A.; Houbrechts, S. *Organometallics* **1996**, *15*, 1935. (b) Houbrechts, S.; Clays, K.; Persoons, A.; Cadierno, V.; Gamasa, M. P.; Gimeno, J. *Organometallics* **1996**, *15*, 5266. (c) Wu, I.-Y.; Lin, J. T.; Luo, J.; Sun, S.-S.; Li, C.-S.; Kuan, J. L.; Tsai, C.; Hsu, C.-C.; Lin, J.-L. *Organometallics* **1997**, *16*, 2038.

(10) Tamm, M.; Jentzsch, T.; Werncke, W. *Organometallics* **1997**, *16*, 1418.

(11) (a) Clays, K.; Persoons, A. *Phys. Rev. Lett*. **1991**, *66*, 2980. (b) Clays, K.; Persoons, A. *Rev. Sci. Instrum*. **1992**, *63*, 3285. (c) Hendrickx, E.; Clays, K.; Persoons, A.; Dehu, C.; Brédas, J. L. *J. Am. Chem. Soc*. **1995**, *117*, 3547.

(12) Coe, B. J.; Chamberlain, M. C.; Essex-Lopresti, J. P.; Gaines, S.; Jeffery, J. C.; Houbrechts, S.; Persoons, A. *Inorg. Chem*. **1997**, *36*, 3284.

(13) Kuzuya, M.; Kondo, S.; Murase, K. *J. Phys. Chem*. **1993**, *97*, 7800.

(14) See, for example: (a) Marder, S. R.; Perry, J. W.; Yakymyshyn, C. P. *Chem. Mater*. **1994**, *6*, 1137. (b) Chauchard, E.; Combellas, C.; Hendrickx, E.; Mathey, G.; Suba, C.; Persoons, A.; Thiebault, A. *Chem. Phys. Lett*. **1995**, *238*, 47. (c) Duan, X.-M.; Okada, S.; Oikawa, H.; Matsuda, H.; Nakanishi, H. *Mol. Cryst. Liq. Cryst*. **1995**, *267*, 89.

(15) Coe, B. J.; Essex-Lopresti, J. P.; Harris, J. A.; Houbrechts, S.; Persoons, A. *Chem. Commun.* **1997**, 1645.

(16) Curtis, J. C.; Sullivan, B. P.; Meyer, T. J. *Inorg. Chem*. **1983**, *22*, 224.

(500 mg, 1.29 mmol) and 4-aminoacetophenone (1.88 g, 13.9 mmol) in ethanol (100 mL) was heated at reflux for 50 h. The solvent was reduced to a small volume in vacuo, water was added, and the precipitate of 2,4-dinitroaniline was filtered off and washed with water. The aqueous filtrate was evaporated to a small volume, acetone was added, and the solution was stored in a refrigerator for 24 h. The pale golden microcrystalline product was filtered off, washed with acetone, and dried: 360 mg, 81%; δ_H (D_2O) 9.23 (2 H, d, $J = 7.0$ Hz, C_5H_4N−AcPh), 8.75 (2 H, br d, $J = 5.9$ Hz, C_5H_4N), 8.56 (2 H, d, $J = 7.0$ Hz, C_5H_4N−AcPh), 8.25 (2 H, d, $J = 8.8$ Hz, C_6H_4−Ac), 7.95 (2 H, d, $J = 6.3$ Hz, C_5H_4N), 7.90 (2 H, d, $J = 8.7$ Hz, C_6H_4−Ac), 2.69 (3 H, s, Ac); ν(C═O) 1692 vs cm^{-1}. Anal. Calcd for $C_{18}H_{15}ClN_2O\cdot 2H_2O$: C, 62.34; H, 5.52; N, 8.08; Cl, 10.22. Found: C, 62.35; H, 5.40; N, 7.93; Cl, 10.39.

Data for $[Ru^{II}(NH_3)_5(MeQ^+)](PF_6)_3$ (1): δ_H (CD_3COCD_3) 9.15 (2 H, d, $J = 7.0$ Hz, C_5H_4N−Me), 9.04 (2 H, d, $J = 6.9$ Hz, C_5H_4N), 8.68 (2 H, d, $J = 7.0$ Hz, C_5H_4N−Me), 7.87 (2 H, d, $J = 7.1$ Hz, C_5H_4N), 4.53 (3 H, s, Me), 3.50 (3 H, s, *trans*-NH_3), 2.66 (12 H, s, 4 × *cis*-NH_3). Anal. Calcd for $C_{11}H_{26}F_{18}N_7P_3Ru\cdot 0.2C_3H_6O$: C, 17.33; H, 3.41; N, 12.20. Found: C, 17.31; H, 3.01; N, 12.57.

Data for $[Ru^{II}(NH_3)_5(PhQ^+)](PF_6)_3$ (2). Indigo solid: 73%; δ_H (CD_3COCD_3) 9.33 (2 H, d, $J = 7.2$ Hz, C_5H_4N−Ph), 9.21 (2 H, d, $J = 7.1$ Hz, C_5H_4N), 8.86 (2 H, d, $J = 7.3$ Hz, C_5H_4N−Ph), 8.01−7.94 (4 H, c m, C_5H_4N and Ph), 7.84−7.78 (3 H, c m, Ph), 3.60 (3 H, s, *trans*-NH_3), 2.70 (12 H, s, 4 × *cis*-NH_3). Anal. Calcd for $C_{16}H_{28}F_{18}N_7P_3Ru\cdot 0.5C_3H_6O$: C, 23.79; H, 3.54; N, 11.10. Found: C, 23.60; H, 3.39; N, 11.19.

Data for $[Ru^{II}(NH_3)_5(4\text{-}AcPhQ^+)](PF_6)_3$ (3). Indigo solid: 35%; δ_H (CD_3COCD_3) 9.40 (2 H, d, $J = 7.2$ Hz, C_5H_4N−Ph-4-Ac), 9.22 (2 H, d, $J = 7.0$ Hz, C_5H_4N), 8.89 (2 H, d, $J = 7.2$ Hz, C_5H_4N−Ph-4-Ac), 8.35 (2 H, d, $J = 8.8$ Hz, C_6H_4−Ac), 8.15 (2 H, d, $J = 8.8$ Hz, C_6H_4−Ac), 7.97 (2 H, d, $J = 7.1$ Hz, C_5H_4N), 3.64 (3 H, s, *trans*-NH_3), 2.72 (15 H, s, 4 × *cis*-NH_3 and Ac); ν(C═O) 1681 m cm^{-1}. Anal. Calcd for $C_{18}H_{30}F_{18}N_7OP_3Ru\cdot 0.3C_3H_6O$: C, 24.84; H, 3.51; N, 10.73. Found: C, 24.81; H, 3.29; N, 10.69.

Synthesis of $[Ru^{II}(NH_3)_5(2,4\text{-}DNPhQ^+)](PF_6)_3$ (4). A solution of $[Ru^{II}(NH_3)_5(H_2O)](PF_6)_2$ (250 mg, 0.506 mmol) and [2,4-$DNPhQ^+$]$PF_6\cdot 0.5H_2O$ (238 mg, 0.499 mmol) in acetone (5 mL) was stirred at room temperature for 2 h. The addition of diethyl ether afforded a dark precipitate, which was collected by filtration, washed with diethyl ether, and dried. Purification was effected by precipitation from acetone/aqueous NH_4PF_6 and then from acetone/diethyl ether followed by recrystallization from acetone/dichloromethane to afford a dark purple solid: 101 mg, 21%; δ_H (CD_3COCD_3) 9.37 (2 H, d, $J = 7.2$ Hz, C_5H_4N), 9.28−9.25 (3 H, c m, H^3 and C_5H_4N), 9.02 (1 H, dd, $J_{5,6} = 8.8$ Hz, $J_{3,5} = 2.6$ Hz, H^5), 8.97 (2 H, d, $J = 7.4$ Hz, C_5H_4N), 8.56 (1 H, d, $J_{5,6} = 8.7$ Hz, H^6), 7.98 (2 H, d, $J = 7.0$ Hz, C_5H_4N), 3.74 (3 H, s, *trans*-NH_3), 2.75 (12 H, s, 4 × *cis*-NH_3); $\nu_{as}(NO_2)$ 1547 s, $\nu_s(NO_2)$ 1347 s cm^{-1}. Anal. Calcd for $C_{16}H_{26}F_{18}N_9O_4P_3Ru$: C, 20.35; H, 2.77; N, 13.35. Found: C, 21.09; H, 3.05; N, 13.00.

Synthesis of *trans*-$[Ru^{III}(SO_4)(NH_3)_4(PhQ^+)]Cl_2$ (5). A mixture of *trans*-$[Ru^{II}Cl(NH_3)_4(SO_2)]Cl$ (100 mg, 0.329 mmol) and $[PhQ^+]Cl\cdot 2H_2O$ (200 mg, 0.656 mmol) was dissolved in water (5 mL) and heated at ca. 45 °C under Ar for 30 min. Acetone (25 mL) was added to the dark brown solution, and the mauve precipitate was collected by filtration, washed with acetone, and dried to afford crude *trans*-$[Ru^{II}(NH_3)_4(SO_2)(PhQ^+)]Cl_3$: 180 mg, 96%. This material was then dissolved in water (ca. 10 mL) and oxidized by the addition of a 1/1 mixture of 30% aqueous H_2O_2 solution/2 M HCl (3 mL). After 5 min at room temperature, acetone (100 mL) was added to the yellow solution and the golden precipitate was collected by filtration, washed with acetone, and dried: 165 mg, 92%. The same quantity of this crude product was used in the subsequent syntheses of **7**−**10**.

Synthesis of *trans*-$[Ru^{III}(SO_4)(NH_3)_4(4\text{-}AcPhQ^+)]Cl_2$ (6). This was prepared similarly to **5** by using $[4\text{-}AcPhQ^+]Cl\cdot 2H_2O$ (229 mg, 0.660 mmol) in place of $[PhQ^+]Cl\cdot 2H_2O$ to afford a golden solid: 155 mg, 77%. The same quantity of this crude product was used in the subsequent syntheses of **11**−**14**.

Synthesis of *trans*-$[Ru^{II}(NH_3)_4(PhQ^+)(dmap)](PF_6)_3$ (7). A solution of **5** (165 mg, 0.290 mmol) in water (10 mL) was reduced over zinc amalgam (5 lumps) with Ar agitation for 5 min. This was then filtered under Ar into a flask containing 4-(dimethylamino)pyridine (dmap; 175 mg, 1.43 mmol), and the solution was stirred at room temperature in the dark under Ar for 3 h. The addition of aqueous NH_4PF_6 to the deep purple solution gave a dark precipitate, which was collected by filtration, washed with water, and dried. The product was purified by precipitation from acetone/$[NBu_4]Cl$ followed by precipitation from water/aqueous NH_4PF_6 to afford a dark indigo solid: 169 mg, 61%; δ_H (CD_3COCD_3) 9.38 (2 H, d, $J = 7.1$ Hz, C_5H_4N−Ph), 9.14 (2 H, d, $J = 7.0$ Hz, C_5H_4N), 8.86 (2 H, d, $J = 7.1$ Hz, C_5H_4N−Ph), 8.34 (2 H, d, $J = 7.2$ Hz, NC_5H_4−NMe_2), 8.06 (2 H, d, $J = 7.0$ Hz, C_5H_4N), 8.02−7.98 (2 H, c m, Ph), 7.82−7.79 (3 H, c m, Ph), 6.88 (2 H, d, $J = 7.2$ Hz, NC_5H_4−NMe_2), 3.17 (6 H, s, NMe_2), 2.78 (12 H, s, 4 × NH_3). Anal. Calcd for $C_{23}H_{35}F_{18}N_8P_3Ru$: C, 28.79; H, 3.68; N, 11.68. Found: C, 29.08; H, 3.43; N, 11.92.

Synthesis of *trans*-$[Ru^{II}(NH_3)_4(PhQ^+)(mim)](PF_6)_3$ (8). This was prepared and purified identically to **7** by using 1-methylimidazole (mim; 0.2 mL, 2.49 mmol) in place of dmap. A dark indigo solid was obtained: 205 mg, 77%; δ_H (CD_3COCD_3) 9.38 (2 H, d, $J = 7.2$ Hz, C_5H_4N−Ph), 9.21 (2 H, d, $J = 7.0$ Hz, C_5H_4N), 8.86 (2 H, d, $J = 7.1$ Hz, C_5H_4N−Ph), 8.24 (1 H, s, im), 8.05−7.97 (4 H, c m, C_5H_4N and Ph), 7.84−7.79 (3 H, c m, Ph), 7.48 (1 H, t, $J = 1.4$ Hz, im), 7.41 (1 H, t, $J = 1.4$ Hz, im), 3.93 (3 H, s, *Me*-im), 2.73 (12 H, s, 4 × NH_3). Anal. Calcd for $C_{20}H_{31}F_{18}N_8P_3Ru$: C, 26.13; H, 3.40; N, 12.19. Found: C, 26.26; H, 3.29; N, 12.11.

Synthesis of *trans*-$[Ru^{II}(NH_3)_4(PhQ^+)(dmabn)](PF_6)_3$ (9). This was obtained in crude form identically to **7** by using 4-(dimethylamino)-benzonitrile (dmabn; 210 mg, 1.44 mmol) in acetone (15 mL) in place of dmap. The product was purified by precipitation from acetone/diethyl ether to afford a dark burgundy solid: 110 mg, 39%; δ_H (CD_3COCD_3) 9.45 (2 H, d, $J = 7.2$ Hz, C_5H_4N−Ph), 9.21 (2 H, d, $J = 6.9$ Hz, C_5H_4N), 8.88 (2 H, d, $J = 7.2$ Hz, C_5H_4N−Ph), 8.15 (2 H, d, $J = 7.0$ Hz, C_5H_4N), 8.02−7.97 (2 H, c m, Ph), 7.85−7.80 (3 H, c m, Ph), 7.68 (2 H, d, $J = 9.1$ Hz, Me_2N−C_6H_4−CN), 6.86 (2 H, d, $J = 9.2$ Hz, Me_2N−C_6H_4−CN), 3.11 (6 H, s, NMe_2), 2.84 (12 H, s, 4 × NH_3). Anal. Calcd for $C_{25}H_{35}F_{18}N_8P_3Ru$: C, 30.53; H, 3.59; N, 11.39. Found: C, 30.54; H, 3.66; N, 11.24.

Synthesis of *trans*-$[Ru^{II}(NH_3)_4(PhQ^+)(PTZ)](PF_6)_3$ (10). A solution of **5** (165 mg, 0.290 mmol) in water (10 mL) was reduced over zinc amalgam (5 lumps) with Ar agitation for 5 min and then filtered under Ar into a flask containing acetone (200 mL). After refrigeration, the deep blue precipitate was collected by filtration, washed with acetone, and dried to yield a turquoise solid (145 mg). This was dissolved in water (5 mL) and added to solid NH_4PF_6 (1.5 g). After refrigeration, the deep purple precipitate was collected by filtration, dried, and then dissolved in acetone (10 mL), and phenothiazine (PTZ; 650 mg, 3.26 mmol) was added. The deep blue solution turned purple within minutes and was stirred in the dark under Ar for 1 h to yield a deep burgundy solution. The addition of diethyl ether afforded a dark precipitate, which was collected by filtration, washed with diethyl ether, and dried. Purification was effected by precipitation from acetone/aqueous NH_4PF_6 and then from acetone/diethyl ether to yield a dark red solid (ca. 95% pure by ^1H NMR): 135 mg, 45%; δ_H (CD_3COCD_3) 9.44 (2 H, d, $J = 7.2$ Hz, C_5H_4N−Ph), 8.93 (2 H, d, $J = 6.9$ Hz, C_5H_4N), 8.80 (2 H, d, $J = 7.1$ Hz, C_5H_4N−Ph), 8.71 (1 H, s, NH), 8.19 (2 H, d, $J = 6.9$ Hz, C_5H_4N), 8.00−7.95 (2 H, c m, Ph), 7.82−7.78 (3 H, c m, Ph), 7.57 (2 H, d, $J = 7.7$ Hz, PTZ), 7.44−7.36 (2 H, m, PTZ), 7.20−7.12 (4 H, m, PTZ), 2.60 (12 H, s, 4 × NH_3). Anal. Calcd for $C_{28}H_{34}F_{18}N_7P_3RuS$: C, 32.44; H, 3.31; N, 9.46; S, 3.09. Found: C, 32.86; H, 3.62; N, 8.94; S, 3.34.

Synthesis of *trans*-$[Ru^{II}(NH_3)_4(4\text{-}AcPhQ^+)(dmap)](PF_6)_3$ (11). This was prepared and purified identically to **7** by using **6** (155 mg, 0.253 mmol) in place of **5**. The product was precipitated once further from acetone/diethyl ether to afford an indigo solid: 158 mg, 62%; δ_H (CD_3COCD_3) 9.43 (2 H, d, $J = 7.2$ Hz, C_5H_4N−Ph-4-Ac), 9.14 (2 H, d, $J = 7.0$ Hz, C_5H_4N), 8.88 (2 H, d, $J = 7.2$ Hz, C_5H_4N−Ph-4-Ac), 8.38−8.32 (4 H, c m, C_6H_4−Ac and NC_5H_4−NMe_2), 8.14 (2 H, d, $J = 8.8$ Hz, C_6H_4−Ac), 8.06 (2 H, d, $J = 7.0$ Hz, C_5H_4N), 6.88 (2 H, d, $J = 7.2$ Hz, NC_5H_4−NMe_2), 3.16 (6 H, s, NMe_2), 2.77 (12 H, s, 4 × NH_3), 2.72 (3 H, s, Ac); ν(C═O) 1686 m cm^{-1}. Anal. Calcd for $C_{25}H_{37}F_{18}N_8OP_3Ru$: C, 29.98; H, 3.72; N, 11.19. Found: C, 29.77; H, 3.86; N, 11.22.

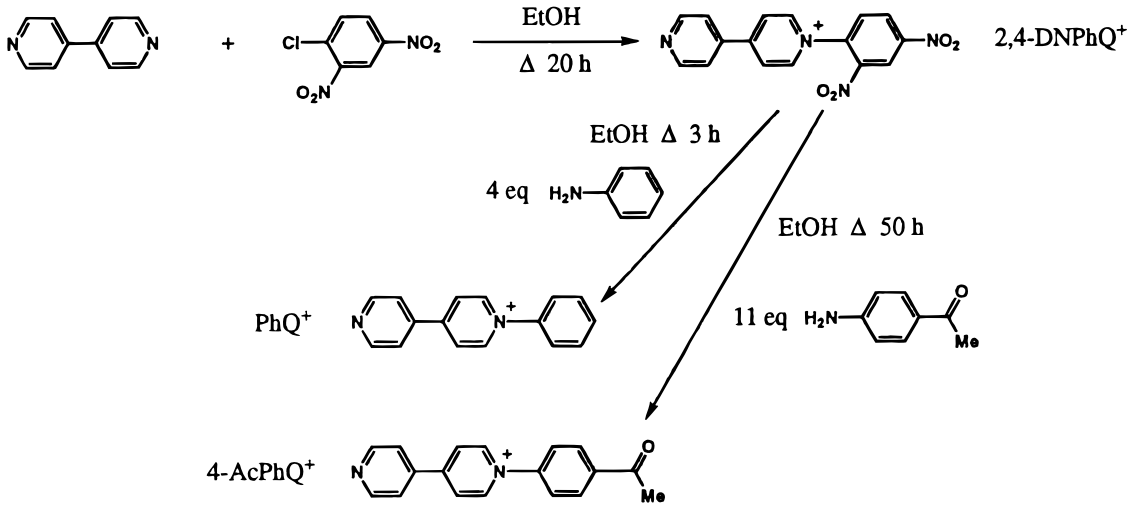

Figure 1. Synthesis of the ligands PhQ^+, 4-$AcPhQ^+$, and 2,4-$DNPhQ^+$.

Synthesis of *trans*-[$Ru^{II}(NH_3)_4$(4-$AcPhQ^+$)(mim)]$(PF_6)_3$ (12). This was prepared and purified identically to **8** by using **6** (155 mg, 0.253 mmol) in place of **5** to afford an indigo solid: 160 mg, 66%; δ_H (CD_3COCD_3) 9.45 (2 H, d, J = 6.7 Hz, C_5H_4N−Ph-4-Ac), 9.23 (2 H, d, J = 6.8 Hz, C_5H_4N), 8.90 (2 H, d, J = 6.6 Hz, C_5H_4N−Ph-4-Ac), 8.36 (2 H, d, J = 8.6 Hz, C_6H_4−Ac), 8.26 (1 H, s, im), 8.15 (2 H, d, J = 8.7 Hz, C_6H_4−Ac), 8.05 (2 H, d, J = 6.8 Hz, C_5H_4N), 7.50 (1 H, s, im), 7.43 (1 H, s, im), 3.94 (3 H, s, *Me*-im), 2.75 (12 H, s, 4 × NH_3), 2.73 (3 H, s, Ac); ν(C═O) 1684 m cm^{-1}. Anal. Calcd for $C_{22}H_{33}F_{18}N_8OP_3Ru$: C, 27.48; H, 3.46; N, 11.65. Found: C, 27.74; H, 3.55; N, 11.75.

Synthesis of *trans*-[$Ru^{II}(NH_3)_4$(4-$AcPhQ^+$)(dmabn)]$(PF_6)_3$ (13). This was prepared and purified identically to **9** by using **6** (155 mg, 0.253 mmol) in place of **5** to afford a purple solid: 161 mg, 62%; δ_H (CD_3COCD_3) 9.51 (2 H, d, J = 7.1 Hz, C_5H_4N−Ph-4-Ac), 9.23 (2 H, d, J = 6.9 Hz, C_5H_4N), 8.92 (2 H, d, J = 7.1 Hz, C_5H_4N−Ph-4-Ac), 8.37 (2 H, d, J = 8.8 Hz, C_6H_4−Ac), 8.18−8.13 (4 H, c m, C_5H_4N and C_6H_4−Ac), 7.68 (2 H, d, J = 9.1 Hz, Me_2N−C_6H_4−CN), 6.87 (2 H, d, J = 9.1 Hz, Me_2N−C_6H_4−CN), 3.11 (6 H, s, NMe_2), 2.86 (12 H, s, 4 × NH_3), 2.73 (3 H, s, Ac); ν(C═O) 1686 m cm^{-1}. Anal. Calcd for $C_{27}H_{37}F_{18}N_8OP_3Ru$: C, 31.62; H, 3.64; N, 10.93. Found: C, 31.67; H, 3.80; N, 10.80.

Synthesis of *trans*-[$Ru^{II}(NH_3)_4$(4-$AcPhQ^+$)(PTZ)]$(PF_6)_3$ (14). This was prepared and purified identically to **10** by using **6** (155 mg, 0.253 mmol) in place of **5** to afford a deep red solid: 120 mg, 42%; δ_H (CD_3COCD_3) 9.50 (2 H, d, J = 7.1 Hz, C_5H_4N−Ph-4-Ac), 8.94 (2 H, d, J = 6.8 Hz, C_5H_4N), 8.83 (2 H, d, J = 7.1 Hz, C_5H_4N−Ph-4-Ac), 8.72 (1 H, s, NH), 8.36 (2 H, d, J = 8.8 Hz, C_6H_4−Ac), 8.20 (2 H, d, J = 6.9 Hz, C_5H_4N), 8.14 (2 H, d, J = 8.8 Hz, C_6H_4−Ac), 7.57 (2 H, d, J = 7.7 Hz, PTZ), 7.45−7.37 (2 H, m, PTZ), 7.21−7.13 (4 H, m, PTZ), 2.72 (3 H, s, Ac), 2.61 (12 H, s, 4 × NH_3); ν(C═O) 1685 m cm^{-1}. Anal. Calcd for $C_{30}H_{36}F_{18}N_7OP_3RuS\cdot 2H_2O$: C, 32.32; H, 3.62; N, 8.80; S, 2.88. Found: C, 32.50; H, 3.34; N, 8.86; S, 3.17.

X-ray Structural Determinations. Crystals of $[PhQ^+]Cl\cdot 2H_2O$ were grown by refrigeration of a water/acetone solution, and crystals of *trans*-$[Ru(NH_3)_4(PhQ^+)(PTZ)](PF_6)_3\cdot Et_2O$ (**10**·Et_2O) were grown by diffusion of diethyl ether into an acetone solution containing added PTZ at 4 °C in the dark. Crystallization in the absence of free PTZ leads to decomposition and production of a blue material.

Platelike crystals of $[PhQ^+]Cl\cdot 2H_2O$ (yellow) and **10**·Et_2O (red), having approximate dimensions of 0.50 × 0.40 × 0.2 mm and 0.20 × 0.20 × 0.02 mm, respectively, were mounted on glass fibers, and data were collected on a Siemens SMART CCD area-detector three-circle diffractometer at low temperature. For three settings of ϕ, narrow data "frames" were collected for 0.3° increments in ω. A total of 2082 and 2132 frames of data were collected, affording a sphere of data for $[PhQ^+]Cl\cdot 2H_2O$ and **10**·Et_2O, respectively. At the end of data collection the first 50 frames were re-collected to establish that crystal decay had not taken place. The substantial redundancy in data allows empirical absorption corrections to be applied using multiple measurements of equivalent reflections. Data frames were collected for 15s/frame for $[PhQ^+]Cl\cdot 2H_2O$ and 30 s/frame for **10**·Et_2O, giving overall data collection times of ca. 14 and ca. 25 h, respectively. The data frames were integrated using SAINT.[17]

The structures were solved by direct methods and refined by full-matrix least squares on all F_o^2 data using Siemens SHELXTL 5.03.[17] All non-hydrogen atoms were refined anisotropically. In the case of $[PhQ^+]Cl\cdot 2H_2O$, the protons of the two water molecules were located and refined with isotropic thermal parameters ca. 1.2 × the equivalent isotropic thermal parameters of their parent oxygen atoms. The NH hydrogen of the PTZ ligand in **10**·Et_2O was located and refined. All other hydrogen atoms were included in calculated positions with isotropic thermal parameters ca. 1.2 × (aromatic CH) or 1.5 × (Me) the equivalent isotropic thermal parameters of their parent carbon atoms. All calculations were carried out on Silicon Graphics Indy or Indigo computers. The asymmetric unit of $[PhQ^+]Cl\cdot 2H_2O$ contains one molecule of the cation, one chloride anion, and two water molecules in general positions. The asymmetric unit of **10**·Et_2O contains one molecule of the cation, three PF_6^- anions, and one molecule of diethyl ether in general positions. The diethyl ether solvent molecule and the anion PF_6^- (P2) were restrained to model perfect geometry.

ORTEP[18] diagrams showing views of $[PhQ^+]Cl\cdot 2H_2O$ and the complex cation in **10**·Et_2O are given in Figures 3 and 4. Crystallographic data and refinement details are presented in Table 3, and selected bond distances and angles in Tables 4 and 5. Additional material available from the Cambridge Crystallographic Data Centre comprises final atomic fractional coordinates, thermal parameters, and nonessential bond lengths and angles.

Hyper-Rayleigh Scattering. Details of the HRS experiment have been discussed previously,[11] and the experimental procedure used was as described recently.[19] β values were obtained by using the electric-field-induced second harmonic generation β_{1064} value for 4-nitroaniline of 29.2 × 10^{-30} esu in acetonitrile[20] as an external reference. All measurements were performed using the 1064 nm fundamental wavelength of an injection-seeded, Q-switched Nd:YAG laser (Quanta-Ray GCR-5, 8 ns pulses, 7 mJ, 10 Hz). Dilute acetonitrile solutions (10^{-4}−10^{-5} M) were used to ensure a linear dependence of $I_{2\omega}/I_\omega^2$ upon solute concentration, precluding the need for Lambert−Beer correction factors. All samples were passed through a 0.45 μm filter (Millipore)

(17) *SHELXTL 5.03 program system*; Siemens Analytical X-ray Instruments: Madison, WI, 1995.
(18) Johnson, C. K. *ORTEP: A Fortran Thermal Ellipsoid Plot Program*; Technical Report ORNL-5138; Oak Ridge National Laboratory: Oak Ridge, TN, 1976.
(19) Houbrechts, S.; Clays, K.; Persoons, A.; Pikramenou, Z.; Lehn, J.-M. *Chem. Phys. Lett.* **1996**, *258*, 485.
(20) Stähelin, M.; Burland, D. M.; Rice, J. E. *Chem. Phys. Lett.* **1992**, *191*, 245.

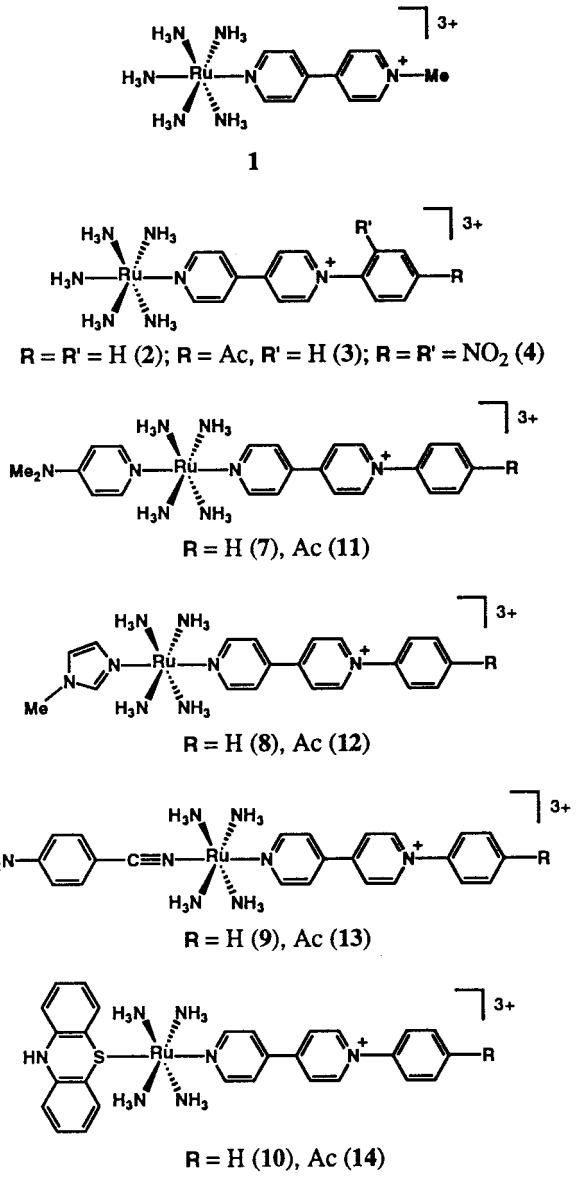

Figure 2. Structures of the complex cations in the salts **1**−**4** and **7**−**14**.

and were checked for fluorescence, which can interfere with the HRS signal.[21−24] One-dimensional hyperpolarizability is assumed, i.e., $\beta_{1064} = \beta_{333}$, and a relative error of ±15% is estimated.

Results and Discussion

Synthetic Studies. The new compounds [PhQ^+]Cl and [2,4-$DNPhQ^+$]Cl were synthesized by using modifications of a literature report for *N*,*N*′-diphenyl-4,4′-bipyridinium dichloride.[25] Nucleophilic attack by stoichiometric 4,4′-bipyridine on 2,4-dinitrochlorobenzene produces [2,4-$DNPhQ^+$]Cl in reasonable yield, and subsequent treatment with aniline affords [PhQ^+]Cl in high yield. Replacement of aniline by 4-aminoacetophenone produces [4-$AcPhQ^+$]Cl in high yield, but an extended reaction time and a larger excess of reagent are required due to the decreased basicity of the attacking nucleophile. Reaction of 4,4′-bipyridine with 2,4-dinitrofluorobenzene was found to be a much less efficient method for the synthesis of the 2,4-$DNPhQ^+$ cation. The syntheses of the new ligands are shown in Figure 1.

The new complex salts **2**−**14** were prepared by using established coordination chemistry based on either $[Ru(NH_3)_5(H_2O)](PF_6)_2$ or *trans*-$[RuCl(NH_3)_4(SO_2)]Cl$,[16,26,27] with previously described[12] and further modifications. Only 2 equiv of [PhQ^+]Cl·$2H_2O$ or [4-$AcPhQ^+$]Cl·$2H_2O$ was used in the syntheses of the intermediates **5** or **6** because the use of a 5-fold excess, as with [MeQ^+]I,[12] leads to precipitation of excess ligand salt together with the *trans*-$[Ru(NH_3)_4(SO_2)(L^A)]Cl_3$ (L^A = PhQ^+ or 4-$AcPhQ^+$) product. This excess ligand subsequently reacts with the intermediate aquo complexes in the reduction stages, causing contamination by symmetric *trans*-$\{Ru(NH_3)_4(L^A)_2\}^{4+}$ products. The use of only 1 equiv of [PhQ^+]Cl·$2H_2O$ or [4-$AcPhQ^+$]Cl·$2H_2O$ leads to incomplete reactions and reduced yields and purities of the final products. The structures of the complexes, except for **5** and **6**, are shown in Figure 2.

UV−**Visible Studies**. Spectra for all of the complex salts, except for the intermediates **5** and **6**, were recorded in acetonitrile, and results are presented in Table 1.

All of the complexes show intense, broad $d\pi(Ru^{II}) \rightarrow \pi^*(L^A)$ metal-to-ligand charge-transfer (MLCT) bands in the region 520−690 nm, the energies of which depend on the electron-donor ability of the Ru center and the electron-acceptor ability of L^A.[28,29] The complexes of dmap or dmabn also show a high-energy, $d\pi(Ru^{II}) \rightarrow \pi^*(L^D)$ band in the region 320−355 nm. Data for the visible MLCT bands are collected in Table 2, together with those for the related MeQ^+ complex salts for purposes of comparison.

For the pentaammine complex series ($L^D = NH_3$), the steady red-shifting of the MLCT maxima shows that the acceptor strength of L^A increases in the order $MeQ^+ < PhQ^+ <$ 4-$AcPhQ^+ <$ 2,4-$DNPhQ^+$. Parallel trends are also observed for the complexes of MeQ^+, PhQ^+, and 4-$AcPhQ^+$ when L^D is dmap, mim, dmabn, or PTZ. Clearly, N-phenylation does indeed cause the anticipated increase in the π-acceptor strength of the 4,4′-bipyridinium ligand, i.e., the ligand-based LUMOs are stabilized by increased delocalization. This effect is further enhanced by the placement of electron-withdrawing acetyl or nitro substituents on the phenyl ring. The average MLCT energy shift produced on replacing MeQ^+ by PhQ^+ is −0.14 eV, while that on going from PhQ^+ to 4-$AcPhQ^+$ is −0.06 eV. With a given L^A, the MLCT energy decreases as the donor strength of L^D increases, in the order PTZ < dmabn < NH_3 < mim < dmap, reflecting the destabilization of the Ru-based HOMOs.[12]

In addition to the MLCT bands, all of the complexes show intense, high-energy bands below 300 nm due to intraligand $\pi \rightarrow \pi^*$ excitations.

Electrochemical Studies. All of the complex salts, except for **5** and **6**, were studied by cyclic voltammetry in acetonitrile, and results are presented in Table 1.

All except for **4** and **10** exhibit reversible or quasi-reversible Ru(III/II) oxidation waves. For a given L^D, the $E_{1/2}$ values are independent of the nature of L^A, showing that the energy of the Ru-based HOMO is determined only by L^D. The donor abilities

(21) Hendrickx, E.; Dehu, C.; Clays, K.; Brédas, J. L.; Persoons, A. *ACS Symp. Ser*. **1995**, *601*, 82.
(22) Flipse, M. C.; de Jonge, R.; Woudenberg, R. H.; Marsman, A. W.; van Walree, C. A.; Jenneskens, L. W. *Chem. Phys. Lett*. **1995**, *245*, 297.
(23) Morrison, I. D.; Denning, R. G.; Laidlaw, W. M.; Stammers, M. A. *Rev. Sci. Instrum*. **1996**, *67*, 1445.
(24) Stadler, S.; Bourhill, G.; Bräuchle, C. *J. Phys. Chem*. **1996**, *100*, 6927.
(25) Emmert, B.; Roh, N. *Ber. Dtsch. Chem. Ges*. **1925**, *58*, 503.
(26) Tfouni, E.; Ford, P. C. *Inorg. Chem*. **1980**, *19*, 72.
(27) Chang, J. P.; Fung, E. Y.; Curtis, J. C. *Inorg. Chem*. **1986**, *25*, 4233.
(28) Ford, P.; Rudd, De F. P.; Gaunder, R.; Taube, H. *J. Am. Chem. Soc*. **1968**, *90*, 1187.
(29) Johnson, C. R.; Shepherd, R. E. *Inorg. Chem*. **1983**, *22*, 2439.

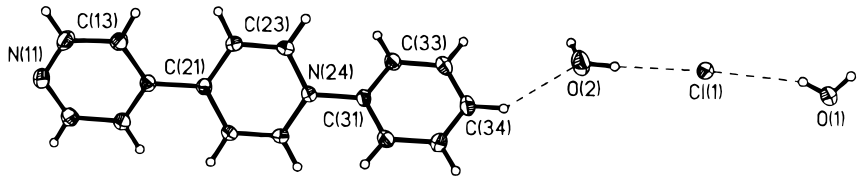

Figure 3. Structural representation of the salt $[PhQ^+]Cl\cdot 2H_2O$. The thermal ellipsoids correspond to 50% probability.

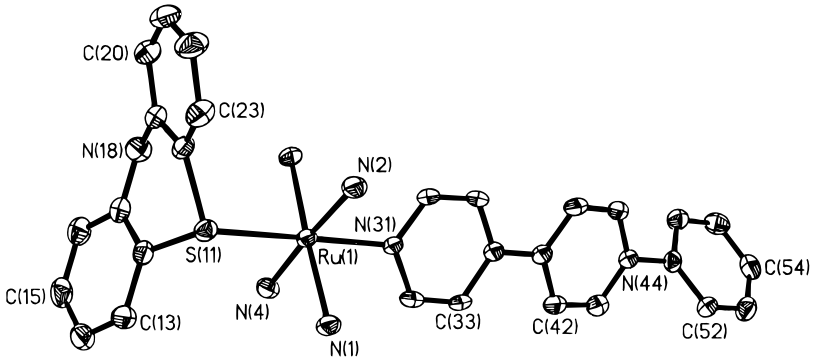

Figure 4. Structural representation of the cation in $\mathbf{10}\cdot Et_2O$, *trans*-$[Ru(NH_3)_4(PhQ^+)(PTZ)]^{3+}$, with hydrogen atoms omitted. The thermal ellipsoids correspond to 50% probability.

Table 1. UV−Visible and Electrochemical Data in Acetonitrile

	$E_{1/2}$, V vs SCE (ΔE_p, mV)[a]			
complex salt (no.)	Ru(III/II)	ligand waves	λ_{max}, nm (ϵ, M^{-1} cm^{-1})[b]	assignment
$[Ru(NH_3)_5(MeQ^+)](PF_6)_3$ (**1**)	0.46 (75)	−0.91 (70)	268 (16 300)	$\pi \rightarrow \pi^*$
		−1.52 (70)	590 (15 800)	$d\pi \rightarrow \pi^*$ (MeQ^+)
$[Ru(NH_3)_5(PhQ^+)](PF_6)_3$ (**2**)	0.46 (75)	−0.75 (70)	280 (18 500)	$\pi \rightarrow \pi^*$
		−1.35 (70)	628 (19 300)	$d\pi \rightarrow \pi^*$ (PhQ^+)
$[Ru(NH_3)_5(4\text{-}AcPhQ^+)](PF_6)_3$ (**3**)	0.47 (80)	−0.64 (75)	286 (20 300)	$\pi \rightarrow \pi^*$
		−1.17 (155)[c]	654 (18 000)	$d\pi \rightarrow \pi^*$ (4-$AcPhQ^+$)
$[Ru(NH_3)_5(2,4\text{-}DNPhQ^+)](PF_6)_3$ (**4**)	0.46[d]	−0.40[e]	270 (25 500)	$\pi \rightarrow \pi^*$
			660 (16 900)	$d\pi \rightarrow \pi^*$ (2,4-$DNPhQ^+$)
trans-$[Ru(NH_3)_4(PhQ^+)(dmap)](PF_6)_3$ (**7**)	0.46 (75)	−0.73 (70)	266 (24 000)	$\pi \rightarrow \pi^*$
		−1.32 (70)	ca. 352 (8400)	$d\pi \rightarrow \pi^*$ (dmap)
			658 (20 000)	$d\pi \rightarrow \pi^*$ (PhQ^+)
trans-$[Ru(NH_3)_4(PhQ^+)(mim)](PF_6)_3$ (**8**)	0.46 (70)	−0.73 (70)	280 (21 400)	$\pi \rightarrow \pi^*$
		−1.34 (70)	648 (21 500)	$d\pi \rightarrow \pi^*$ (PhQ^+)
trans-$[Ru(NH_3)_4(PhQ^+)(dmabn)](PF_6)_3$ (**9**)	0.69 (70)	−0.69 (70)	256 (16 800)	$\pi \rightarrow \pi^*$
		−1.26 (70)	290 (31 400)	$\pi \rightarrow \pi^*$
		1.30 (85)	326 (29 200)	$d\pi \rightarrow \pi^*$ (dmabn)
			572 (19 700)	$d\pi \rightarrow \pi^*$ (PhQ^+)
trans-$[Ru(NH_3)_4(PhQ^+)(PTZ)](PF_6)_3$ (**10**)	0.85 (200)	−0.64 (75)	244 (21 900)	$\pi \rightarrow \pi^*$
		−1.19 (70)	254 (20 700)	$\pi \rightarrow \pi^*$
			284 (22 500)	$\pi \rightarrow \pi^*$
			526 (10 200)	$d\pi \rightarrow \pi^*$ (PhQ^+)
trans-$[Ru(NH_3)_4(4\text{-}AcPhQ^+)(dmap)](PF_6)_3$ (**11**)	0.47 (75)	−0.63 (75)	282 (23 000)	$\pi \rightarrow \pi^*$
		−1.17 (80)	ca. 352 (7600)	$d\pi \rightarrow \pi^*$ (dmap)
			688 (18 600)	$d\pi \rightarrow \pi^*$ (4-$AcPhQ^+$)
trans-$[Ru(NH_3)_4(4\text{-}AcPhQ^+)(mim)](PF_6)_3$ (**12**)	0.48 (75)	−0.63 (70)	286 (23 000)	$\pi \rightarrow \pi^*$
		−1.16 (120)[c]	666 (19 500)	$d\pi \rightarrow \pi^*$ (4-$AcPhQ^+$)
trans-$[Ru(NH_3)_4(4\text{-}AcPhQ^+)(dmabn)](PF_6)_3$ (**13**)	0.70 (80)	−0.60 (70)	290 (40 600)	$\pi \rightarrow \pi^*$
		−1.12 (70)	320 (32 800)	$d\pi \rightarrow \pi^*$ (dmabn)
		1.33 (110)[c]	586 (21 800)	$d\pi \rightarrow \pi^*$ (4-$AcPhQ^+$)
trans-$[Ru(NH_3)_4(4\text{-}AcPhQ^+)(PTZ)](PF_6)_3$ (**14**)	0.87 (90)	−0.56 (70)	258 (23 000)	$\pi \rightarrow \pi^*$
		−1.07 (70)	286 (28 500)	$\pi \rightarrow \pi^*$
			538 (9800)	$d\pi \rightarrow \pi^*$ (4-$AcPhQ^+$)

[a] Measured in solutions ca. 10^{-3} M in analyte and 0.1 M in $[N(C_4H_9\text{-}n)_4]PF_6$ at a Pt bead working electrode with a scan rate of 200 mV s^{-1}. Ferrocene internal reference $E_{1/2} = 0.41$ V, $\Delta E_p = 70$ mV. [b] Solutions $1-4 \times 10^{-5}$ M. [c] Irreversible process as evidenced by $i_{pc} \neq i_{pa}$. [d] E_{pa} for an irreversible oxidation process. [e] E_{pc} for an irreversible reduction process.

of NH_3, dmap, and mim are sufficiently similar to give indistinguishable Ru(III/II) potentials, but the considerably less basic dmabn or PTZ ligands produce rather more positive $E_{1/2}$ values. The essentially irreversible oxidative behavior of **10** is similar to that previously observed for its MeQ^+ analogue, but **14** shows quasi-reversible behavior. The complexes in **9** and **13** each exhibit an additional, quasi-reversible wave assigned to oxidation of the dmabn ligands.

Rather more useful information is gained from examination of the ligand-based reduction waves. These data are collected in Table 2, together with those for the previously reported MeQ^+ complex salts.[12] In each complex, with the exception of **4**, the

Table 2. Visible Absorption, Ligand Reduction, and HRS Data for the Salts *trans*-$[Ru^{II}(NH_3)_4(L^D)(L^A)](PF_6)_3$ in Acetonitrile

no.	L^D	L^A	λ_{max}[MLCT], nm (ϵ, M^{-1} cm^{-1})	E_{max}[MLCT], eV	$E_{1/2}$, V vs SCE $L^{A+/0}$	$E_{1/2}$, V vs SCE $L^{A0/-}$	$\beta_{1064}{}^a \times 10^{30}$ esu	$\beta_0{}^a \times 10^{30}$ esu
1	NH_3	MeQ^+	590 (15 800)	2.10	−0.91	−1.52	750	123
2	NH_3	PhQ^+	628 (19 300)	1.97	−0.75	−1.35	858	220
3	NH_3	4-$AcPhQ^+$	654 (18 000)	1.90	−0.64	−1.17	1112	354
4	NH_3	2,4-$DNPhQ^+$	660 (16 900)	1.88	*b*	*b*	871	289
c	dmap	MeQ^+	614 (17 200)	2.02	−0.87	−1.46	587	130
7	dmap	PhQ^+	658 (20 000)	1.88	−0.73	−1.32	794	260
11	dmap	4-$AcPhQ^+$	688 (18 600)	1.80	−0.63	−1.17	1048	410
c	mim	MeQ^+	602 (16 200)	2.06	−0.88	−1.48	523	100
8	mim	PhQ^+	648 (21 500)	1.91	−0.73	−1.34	874	266
12	mim	4-$AcPhQ^+$	666 (19 500)	1.86	−0.63	−1.16	962	332
c	dmabn	MeQ^+	540 (17 700)	2.30	−0.85	−1.43	621	14
9	dmabn	PhQ^+	572 (19 700)	2.17	−0.69	−1.26	1273	141
13	dmabn	4-$AcPhQ^+$	586 (21 800)	2.12	−0.60	−1.12	1214	180
c	PTZ	MeQ^+	498 (8400)	2.49	−0.80	−1.32	419	40
10	PTZ	PhQ^+	526 (10 200)	2.36	−0.64	−1.19	698	12
14	PTZ	4-$AcPhQ^+$	538 (9800)	2.30	−0.56	−1.07	727	12

[a] β_{1064} is the uncorrected first hyperpolarizability measured using a 1064 nm Nd:YAG laser fundamental; β_0 is the static hyperpolarizability estimated by using the two-level model.[31] The quoted cgs units (esu) can be converted into SI units (C^3 m^3 J^{-2}) by dividing by a factor of 2.693×10^{20}. [b] Irreversible. [c] Reference 12.

Table 3. Crystallographic Data and Refinement Details for $[PhQ^+]Cl\cdot 2H_2O$ and **10**·Et_2O

	$[PhQ^+]Cl\cdot 2H_2O$	**10**·Et_2O
empirical formula	$C_{16}H_{17}ClN_2O_2$	$C_{32}H_{44}F_{18}N_7OP_3RuS$
M_r	304.77	1110.78
cryst syst	triclinic	triclinic
space group	$P\bar{1}$	$P\bar{1}$
a, Å	7.675(2)	10.310(3)
b, Å	9.895(2)	10.698(2)
c, Å	10.175(2)	20.986(4)
α, deg	96.003(1)	95.09(2)
β, deg	104.74(2)	91.49(2)
γ, deg	90.398(1)	105.53(2)
V, $Å^3$	742.7(3)	2218.3(8)
Z	2	2
D_c, g cm^{-3}	1.363	1.663
T, °C	−100(2)	−100(2)
λ, Å	0.710 73 (Mo Kα)	0.710 73 (Mo Kα)
F(000)	320	1120
μ, cm^{-1}	0.263	0.622
scan type	*φ*	*φ*
θ range	2.07−27.47°	1.95−27.48°
h,k,l ranges	−9/9, −12/12, −13/13	−13.13, −13/13, −27/27
no. of reflns collected	7592	23 184
no. of unique reflns (R_{int})	3353 (0.0207)	10 055 (0.0459)
data, restraints, parameters	3352, 0, 202	10 054, 52, 577
final *R* indices $[I > 2\sigma(I)]^{a,b}$	$R_1 = 0.0322$, $wR_2 = 0.0865$	$R_1 = 0.0532$, $wR_2 = 0.1281$
weighting factors $(x, y)^b$	0.0537, 0	0.0735, 0
goodness of fit, *S*	0.971	1.022
peak and hole, e $Å^{-3}$	0.247, −0.245	1.205, −0.692

[a] Structure was refined on F_o^2 using all data; the value of R_1 is given for comparison with older refinements based on F_o with a typical threshold of $F_o > 4\sigma(F_o)$. [b] $wR_2 = [\Sigma w(F_o^2 - F_c^2)^2/\Sigma w(F_o^2)^2]^{1/2}$; $S = [\Sigma w(F_o^2 - F_c^2)^2/(M - N)]^{1/2}$ where M = number of reflections and N = number of parameters; $w^{-1} = [\sigma^2(F_o^2) + (xP)^2 + yP]$ and $P = [\max(F_o^2, 0) + 2F_c^2]/3$.

4,4′-bipyridinium ligands give rise to two reversible or quasi-reversible, one-electron-reduction waves assigned to the $L^{A+/0}$ and $L^{A0/-}$ redox couples. For a given L^D, both of these potentials become less negative in the order $MeQ^+ < PhQ^+ <$ 4-$AcPhQ^+$, confirming the stabilization of the ligand-based LUMOs shown in the visible absorption spectra (vide supra). Replacement of the methyl substituent of MeQ^+ by phenyl produces average positive shifts of 150 mV in both potentials, while substitution of the phenyl ring with a 4-acetyl group produces average positive shifts of 100 and 150 mV in the first and second reduction potentials, respectively. As expected, these shifts for the first reduction potentials correlate reasonably well with the changes in the MLCT maximum energies (vide supra).

Structural Determinations. Single-crystal X-ray structures were obtained for $[PhQ^+]Cl\cdot 2H_2O$ and **10**·Et_2O. Representations of $[PhQ^+]Cl\cdot 2H_2O$ and the cation in **10**·Et_2O are shown in Figures 3 and 4.

The cation in $[PhQ^+]Cl\cdot 2H_2O$ adopts a twisted conformation, with torsion angles C(13)−C(14)-C(21)−C(22) = −19.8° and C(23)−N(24)−C(31)−C(32) = −39.7°. Hydrogen bonding is observed between the aromatic hydrogen H(34) of the PhQ^+ cation and the oxygen atom O(2) of one of the water molecules, with a bond length of 2.392 Å. Hydrogen bonding is also

Table 4. Selected Bond Distances (Å) and Angles (deg) for $[PhQ^+]Cl\cdot 2H_2O$

N(11)−C(16)	1.334(2)	C(23)−N(24)	1.358(2)
N(11)−C(12)	1.345(2)	N(24)−C(25)	1.356(2)
C(12)−C(13)	1.386(2)	N(24)−C(31)	1.460(2)
C(13)−C(14)	1.387(2)	C(25)−C(26)	1.374(2)
C(14)−C(15)	1.398(2)	C(31)−C(36)	1.388(2)
C(14)−C(21)	1.487(2)	C(31)−C(32)	1.389(2)
C(15)−C(16)	1.385(2)	C(32)−C(33)	1.388(2)
C(21)−C(26)	1.394(2)	C(33)−C(34)	1.386(2)
C(21)−C(22)	1.402(2)	C(34)−C(35)	1.388(2)
C(22)−C(23)	1.373(2)	C(35)−C(36)	1.389(2)
C(16)−N(11)−C(12)	116.26(12)	C(25)−N(24)−C(23)	120.24(11)
N(11)−C(12)−C(13)	123.59(13)	C(25)−N(24)−C(31)	119.59(11)
C(12)−C(13)−C(14)	119.61(12)	C(23)−N(24)−C(31)	120.16(10)
C(13)−C(14)−C(15)	117.20(12)	N(24)−C(25)−C(26)	120.35(12)
C(13)−C(14)−C(21)	121.80(11)	C(25)−C(26)−C(21)	121.00(11)
C(15)−C(14)−C(21)	121.00(12)	C(36)−C(31)−C(32)	121.94(12)
C(16)−C(15)−C(14)	118.91(13)	C(36)−C(31)−N(24)	118.97(11)
N(11)−C(16)−C(15)	124.39(12)	C(32)−C(31)−N(24)	119.09(12)
C(26)−C(21)−C(22)	117.21(12)	C(33)−C(32)−C(31)	118.69(13)
C(26)−C(21)−C(14)	121.31(11)	C(34)−C(33)−C(32)	120.26(12)
C(22)−C(21)−C(14)	121.47(12)	C(33)−C(34)−C(35)	120.22(13)
C(23)−C(22)−C(21)	120.41(12)	C(34)−C(35)−C(36)	120.48(13)
N(24)−C(23)−C(22)	120.78(11)	C(31)−C(36)−C(35)	118.41(12)

Table 5. Selected Bond Distances (Å) and Angles (deg) for **10**·Et_2O

Ru(1)−N(1)	2.146(3)	Ru(1)−N(4)	2.139(3)
Ru(1)−N(2)	2.140(3)	Ru(1)−N(31)	2.097(3)
Ru(1)−N(3)	2.144(3)	Ru(1)−S(11)	2.3350(12)
N(1)−Ru(1)−N(2)	85.75(14)	N(3)−Ru(1)−N(4)	88.30(13)
N(1)−Ru(1)−N(3)	177.50(13)	N(3)−Ru(1)−N(31)	88.38(13)
N(1)−Ru(1)−N(4)	93.21(14)	N(3)−Ru(1)−S(11)	92.31(9)
N(1)−Ru(1)−N(31)	89.69(13)	N(4)−Ru(1)−N(31)	87.59(13)
N(1)−Ru(1)−S(11)	89.62(10)	N(4)−Ru(1)−S(11)	92.53(10)
N(2)−Ru(1)−N(3)	92.65(14)	N(31)−Ru(1)−S(11)	179.31(9)
N(2)−Ru(1)−N(4)	176.79(13)	C(12)−S(11)−Ru(1)	111.19(14)
N(2)−Ru(1)−N(31)	89.37(14)	C(24)−S(11)−Ru(1)	109.42(14)
N(2)−Ru(1)−S(11)	90.49(11)	C(12)−S(11)−C(24)	98.0(2)

observed between the hydrogen atom H(2B), the anion Cl(1), and hydrogen atom H(1B). The lengths of the hydrogen bonds Cl(1)−H(1B) and Cl(1)−H(2B) are 2.535 and 2.363 Å, respectively. This is the first *N*-phenyl-4,4′-bipyridinium compound and only the second hetero-*p*-terphenyl analogue to be structurally characterized. The recently reported structure of borabenzene-4-phenylpyridine shows a twisted conformation similar to that of $[PhQ^+]Cl\cdot 2H_2O$.[30]

The structure of the complex in **10**·Et_2O resembles that of its MeQ^+ analogue.[12] In the latter the torsion angle between the two pyridyl rings of the MeQ^+ ligand is 9.6°, whereas in **10**·Et_2O the equivalent angle is only 2.6°. This compares with 19.8° in $[PhQ^+]Cl\cdot 2H_2O$. These data indicate that the extent of electronic delocalization between the two pyridyl rings in the solid state is greater in **10**·Et_2O than in its MeQ^+ analogue, and that complexation of the PhQ^+ ligand enhances inter-ring electronic coupling. The twisting between the phenyl and pyridinium rings in **10**·Et_2O is similar to that in $[PhQ^+]Cl\cdot 2H_2O$, with the C(45)−N(44)−C(51)−C(52) torsion angle being 135°.

Nonlinear Optical Studies. The first hyperpolarizabilities β of the new complexes were measured in acetonitrile using the HRS technique[11,19] with a 1064 nm Nd:YAG laser fundamental. Static hyperpolarizabilities were obtained by application of the two-level model,[31] and results are presented in Table 2. The β_0 values for **10** and **14** are grossly underestimated because a neglect of damping renders the two-level model invalid when the absorption maximum is sufficiently close to the second-harmonic frequency (532 nm).

The large resonance-enhanced β values obtained are comparable to those previously reported for ruthenium organometallics.[9,10] More significantly, the β_0 values are also extremely large and those for the 4-$AcPhQ^+$ complexes in **3**, **11**, and **12** are somewhat greater than those measured for Ru(II) σ-acetylide complexes, for which the highest value reported to date is 232 $\times 10^{-30}$ esu.[9a] Indeed, the β_0 for **11** of 410 $\times 10^{-30}$ esu is almost the largest yet found for a metal-containing chromophore. Although a substituted $[Ru(bpy)_3]^{2+}$ derivative (bpy = 2,2′-bipyridine) was claimed to possess a β_0 value in excess of 10^{-27} esu,[32] it appears that this observation may be primarily due to two-photon excited luminescence, rather than harmonic scattering.[23] A push−pull arylethynyl zinc porphyrin has a β_0 of 800 $\times 10^{-30}$ esu,[33] but the extent of involvement of the metal in the NLO response of such systems is unclear. Within the realm of purely organic NLO molecules, significantly larger β_0 values have been reported only for donor−acceptor polyenes.[34]

The effects of increasing the acceptor strength of L^A while keeping L^D fixed, observed in the visible absorption spectra (vide supra), are also shown in the β_0 values, which consistently increase in the order $L^A = MeQ^+ < PhQ^+ < 4\text{-}AcPhQ^+$. The single complex of 2,4-$DNPhQ^+$ (**4**) provides an apparent, unexpected exception to this trend, but the difference in β_0 between **4** and **3** may not be significant. A 2,4-dinitrophenyl group is evidently more electron deficient than its 4-acetyl counterpart, so the lower β_0 for **4** can most likely be traced to a reduction in delocalization through the *N*-phenylpyridinium unit arising from the steric effect of the *o*-NO_2 group. The crystallographic studies (vide supra), which indicate that the extent of electronic delocalization within the 4,4′-bipyridinium unit is greater in **10**·Et_2O than in its MeQ^+ analogue, are consistent with the larger β_0 values for the PhQ^+ complexes with respect to their MeQ^+ counterparts.

For a given L^A, although the MLCT energies always decrease in the order $L^D = NH_3 >$ mim > dmap (vide supra), the corresponding differences in the β_0 values are small and no clear trends are evident. This indicates that the presence of a trans N-heterocyclic ligand is not especially important in producing a large hyperpolarizability. It is likely that inter-ligand $\pi-\pi$ coupling occurs through the metal centers,[26,35] but the potential benefits of this in terms of extending the overall conjugation are clearly minor. Furthermore, the dmap complexes exhibit a second, high-energy MLCT transition which opposes the low-energy MLCT process. As indicated by the Ru(III/II) reduction potentials (vide supra), the role of L^D is primarily to determine the amount of electron density at the Ru(II) center and hence its π-donor strength toward L^A.

According to the two-level model,[31] the dominant component of β is proportional to both $\Delta\mu$ (the dipole moment change

(30) Qiao, S.; Hoic, D. A.; Fu, G. C. *Organometallics* **1997**, *16*, 1501.

(31) (a) Oudar, J. L.; Chemla, D. S. *J. Chem. Phys*. **1977**, *66*, 2664. (b) Oudar, J. L. *J. Chem. Phys*. **1977**, *67*, 446. (c) Zyss, J.; Oudar, J. L. *Phys. Rev. A* **1982**, *26*, 2016.

(32) Dhenaut, C.; Ledoux, I.; Samuel, I. D. W.; Zyss, J.; Bourgault, M.; Le Bozec, H. *Nature* **1995**, *374*, 339.

(33) LeCours, S. M.; Guan, H.-W.; DiMagno, S. G.; Wang, C. H.; Therien, M. J. *J. Am. Chem. Soc*. **1996**, *118*, 1497.

(34) See, for example: (a) Blanchard-Desce, M.; Alain, V.; Bedworth, P. V.; Marder, S. R.; Fort, A.; Runser, C.; Barzoukas, M.; Lebus, S.; Wortmann, R. *Chem. Eur. J*. **1997**, *3*, 1091. (b) Hsu, C.-C.; Shu, C.-F.; Huang, T.-H.; Wang, C. H.; Lin, J.-L.; Wang, Y.-K.; Zang, Y.-L. *Chem. Phys. Lett*. **1997**, *274*, 466.

(35) (a) Zwickel, A. M.; Creutz, C. *Inorg. Chem.* **1971**, *10*, 2395. (b) Wishart, J. F.; Zhang, X.; Isied, S. S.; Potenza, J. A.; Schugar, H. J. *Inorg. Chem.* **1992**, *31*, 3179.

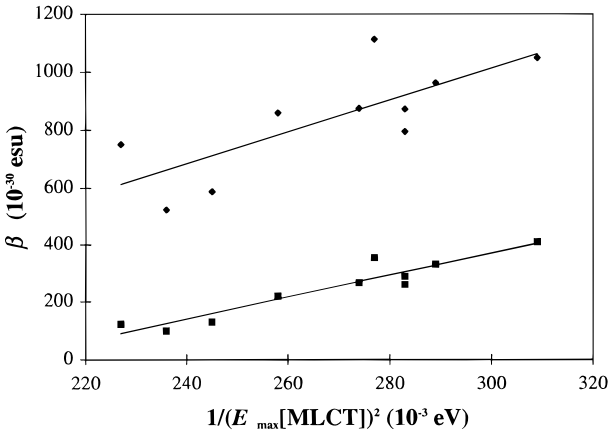

Figure 5. Plot of the first hyperpolarizability against the inverse square of the MLCT energy for the salts **1**−**4**, **7**, **8**, **11**, **12**, and *trans*-[Ru$(NH_3)_4(MeQ^+)(L^D)](PF_6)_3$ (L^D = dmap or mim)[12] (◆ = β; ■ = β_0).

between the ground and excited states) and μ_{ge}^2 (the square of the transition oscillator strength) and inversely proportional to E_{ge}^2 (the square of the energy gap between the two states). A linear correlation between β and $1/E_{ge}^2$ has previously been found for donor−acceptor diphenylacetylenes,[36] indicating that the charge-transfer energy plays a more significant role in determining β than does $\Delta\mu$ or μ_{ge} in such molecules. A similar analysis reveals a relatively poor correlation for β_{1064}, but a much better linear trend for β_0 for the present compounds (Figure 5). The data for the dmabn or PTZ complexes are excluded because their β and β_0 values are less reliable due to the combined effects of resonance enhancement and the limitations of the two-level model. The observed correlation confirms that the visible MLCT excitations are indeed responsible for the large hyperpolarizabilities, as indicated by our earlier results.[12] Furthermore, the product $\Delta\mu(\mu_{ge}^2)$ apparently remains relatively constant within this group of complexes.

(36) Stiegman, A. E.; Graham, E.; Perry, K. J.; Khundkar, L. R.; Cheng, L.-T.; Perry, J. W. *J. Am. Chem. Soc.* **1991**, *113*, 7658.

Conclusions

Dipolar ruthenium(II) tetra- or pentaammine complexes of N-substituted 4,4′-bipyridinium ligands exhibit β_0 values larger than those of most other organotransition metal complexes or organic molecules investigated previously. Intense, low-energy MLCT absorptions are the basis for these extremely large quadratic hyperpolarizabilities which can be tuned by rational changes in ligand structure. We have clearly demonstrated that N-phenylation of 4,4′-bipyridinium ligands is an effective means to increase β_0 in MLCT-based chromophores, and we anticipate that such an approach will also be applicable to purely organic compounds.

It should be emphasized that the properties of these complexes are currently by no means optimized. Present synthetic work includes variations in ligand structures in order to allow the maximization of β_0 and the development of further structure−property correlations. The effects of the conformation of L^A on β_0 and the direct comparison of the donor properties of Ru(II) ammine centers with traditional electron-rich organic groups are of particular interest. The use of Ru(III/II) redox couples as a means to achieve reversible modulation of molecular NLO properties is also an immediate goal. Aspects of importance for potential practical applications such as stability and transparency at relevant wavelengths are also to be addressed.

Acknowledgment. S.H. is a Research Assistant of the Fund for Scientific Research−Flanders. This work was supported by research grants from The Royal Society, from the Belgian National Fund for Scientific Research (G.0308.96), from the Belgian government (IUAP-P4/11), and from the University of Leuven (GOA/1/95). Thanks are due to Johnson Matthey plc for a generous loan of ruthenium trichloride.

Supporting Information Available: Tables of final atomic fractional coordinates, thermal parameters, and nonessential bond lengths and angles (9 pages). Ordering information is given on any current masthead page.

IC971411S